Yamamoto et al., http://www.jcb.org/cgi/content/full/jcb.201202061/DC1

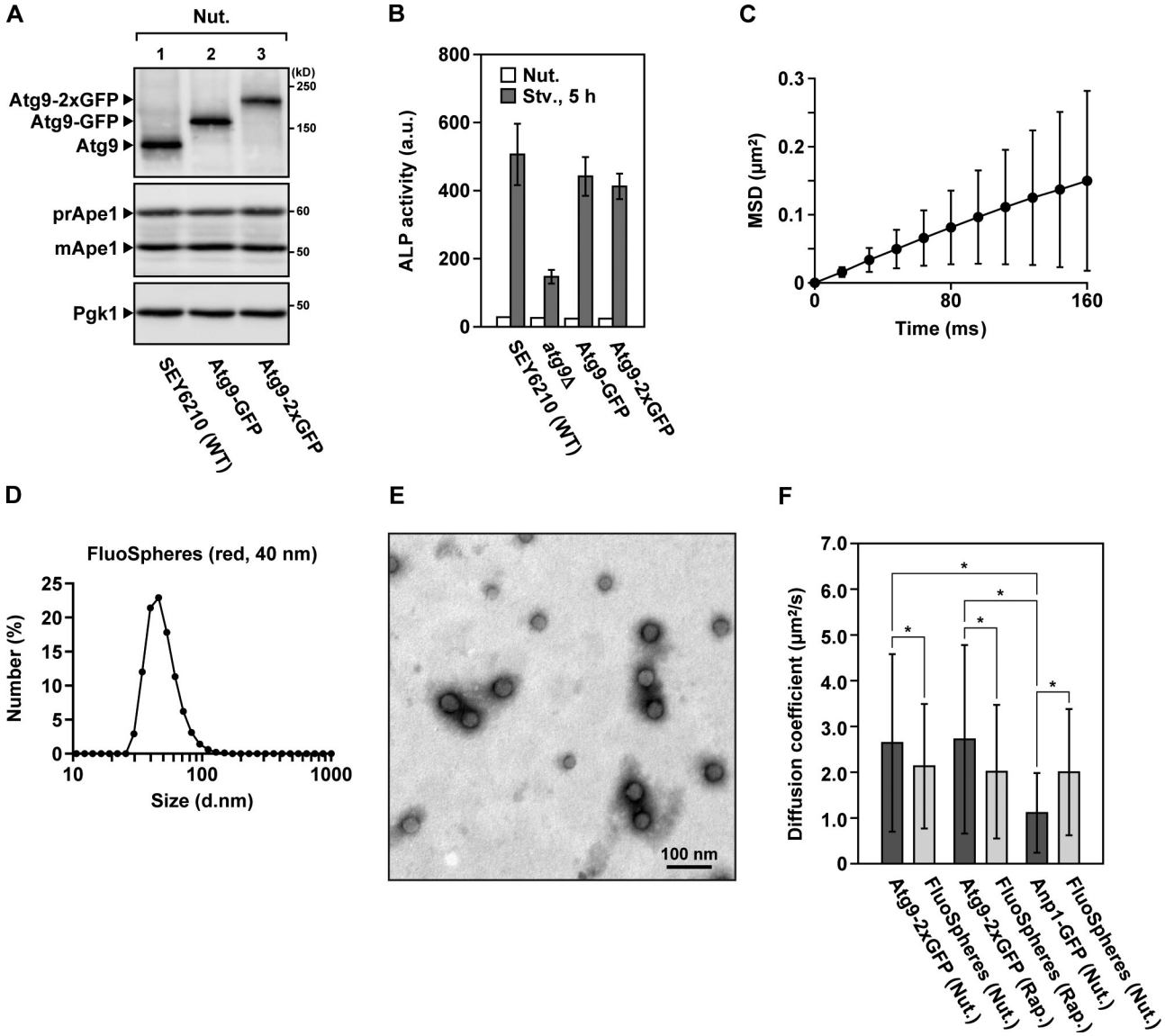

Figure S1. **Atg9-containing structures are observed by high temporal resolution microscopy and analyzed by single-particle tracking.** (A) Total cell lysates were prepared from SEY6210 wild-type cells, *ATG9-GFP* cells, and *ATG9-2×GFP* cells grown in SD/CA medium and then subjected to immunoblotting. (B) Autophagic activities of the cells used in A were measured by alkaline phosphatase (ALP) assay using pTN3 (Noda et al., 1995). Error bars indicate standard deviation. (A and B) The expression level of Atg9-GFP was comparable to that of endogenous Atg9, but that of Atg9-2×GFP was lower than that of endogenous Atg9; however, both Atg9-GFP and Atg9-2×GFP were substantially functional in terms of autophagosome formation as judged by ALP assay, and we also conformed that the intracellular behavior of Atg9-2×GFP puncta appeared to be comparable to that of Atg9-GFP puncta (not depicted). a.u., arbitrary unit; Nut., nutrient; Stv., starved; WT, wild type. (C) Additional data associated with Fig. 1 E. Mean square displacement (MSD) curves calculated from traces of Atg9 puncta in cells starved for 2 h. Error bars indicate standard deviation. (D) Mean size of FluoSpheres used in Fig. 2 A was estimated by DLS. The mean diameter was calculated to be 44.1 nm. d.nm, diameter in nanometers. (E) FluoSpheres used in Fig. 2 A were subjected to negative staining EM. (F) Total MSD curves of the Atg9 puncta in the cells starved for 2 h calculated in Fig. 1 F were shown. Error bars indicate standard deviation. Rap., rapamycin. *, $P < 0.005$.

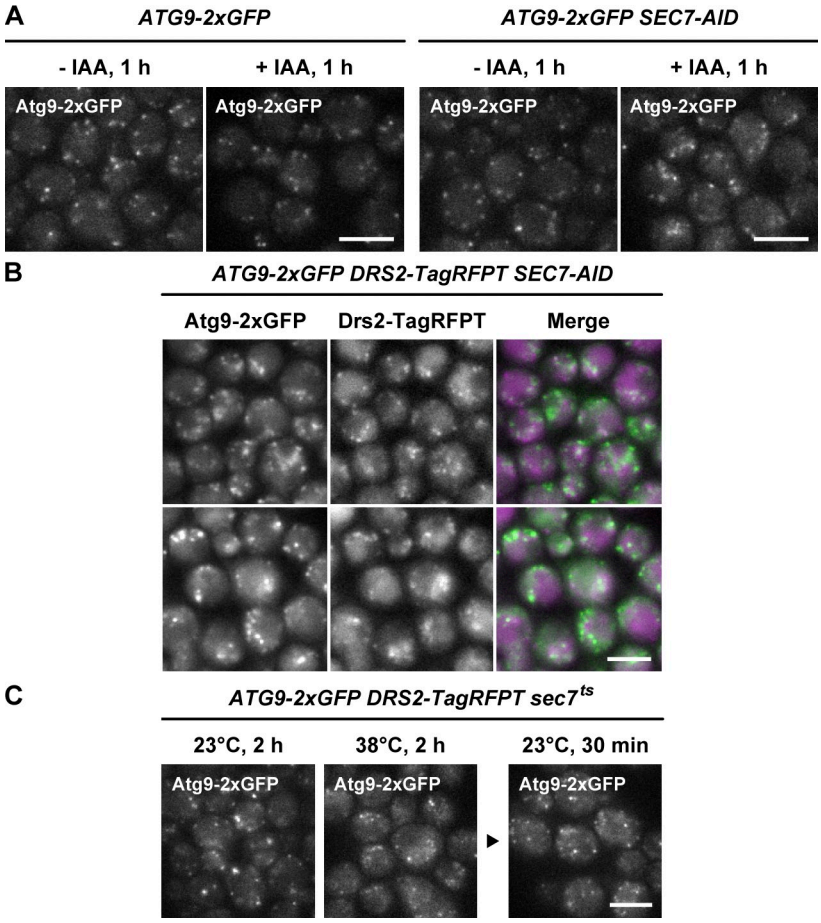

Figure S2. **Atg9 vesicles are derived from the Golgi apparatus.** (A and B) *ATG9-2×GFP DRS2-TagRFPT* cells (wild type) and *ATG9-2×GFP DRS2-TagRFPT SEC7-AID* cells were treated with rapamycin for 30 min and then treated with 500 µg/ml indole-3-acetic acid (IAA) for 1 h. Drs2-TagRFPT was used as a trans-Golgi network marker. Green fluorescence and red fluorescence were acquired concurrently. Sec7 is an essential protein involved in protein trafficking via the Golgi apparatus (Franzusoff and Schekman, 1989), prohibiting the use of an unconditional knockout; therefore, we used an auxin-inducible degron (AID; Nishimura et al., 2009) to allow conditional depletion of Sec7. Upon addition of IAA (a natural auxin), Sec7-AID was degraded in an auxin-dependent manner (not depicted). Concomitantly, a subpopulation of Atg9-2×GFP accumulated at the trans-Golgi network, here labeled with Drs2-TagRFPT (see also Video 3). (C) *ATG9-2×GFP DRS2-TagRFPT sec7^{ts}* cells grown at 23°C were shifted to 38°C and incubated for 2 h. Next, the cells were shifted to 23°C and incubated for 30 min. At the nonpermissive temperature (38°C), Atg9-2×GFP formed immobile structures in *sec7^{ts}* cells (Novick et al., 1980), which were colocalized with Drs2-TagRFPT (not depicted), and after returning to the permissive temperature (23°C), the accumulated Atg9-2×GFP was partially released to the cytoplasm as mobile Atg9 vesicles (see also Video 4). These results are largely consistent with previous studies (Mari et al., 2010; Ohashi and Munro, 2010) and with the hypothesis that the Atg9 vesicles were generated via the Golgi apparatus. The arrowhead indicates temperature shift from 38 to 23°C. Bars, 5 µm.

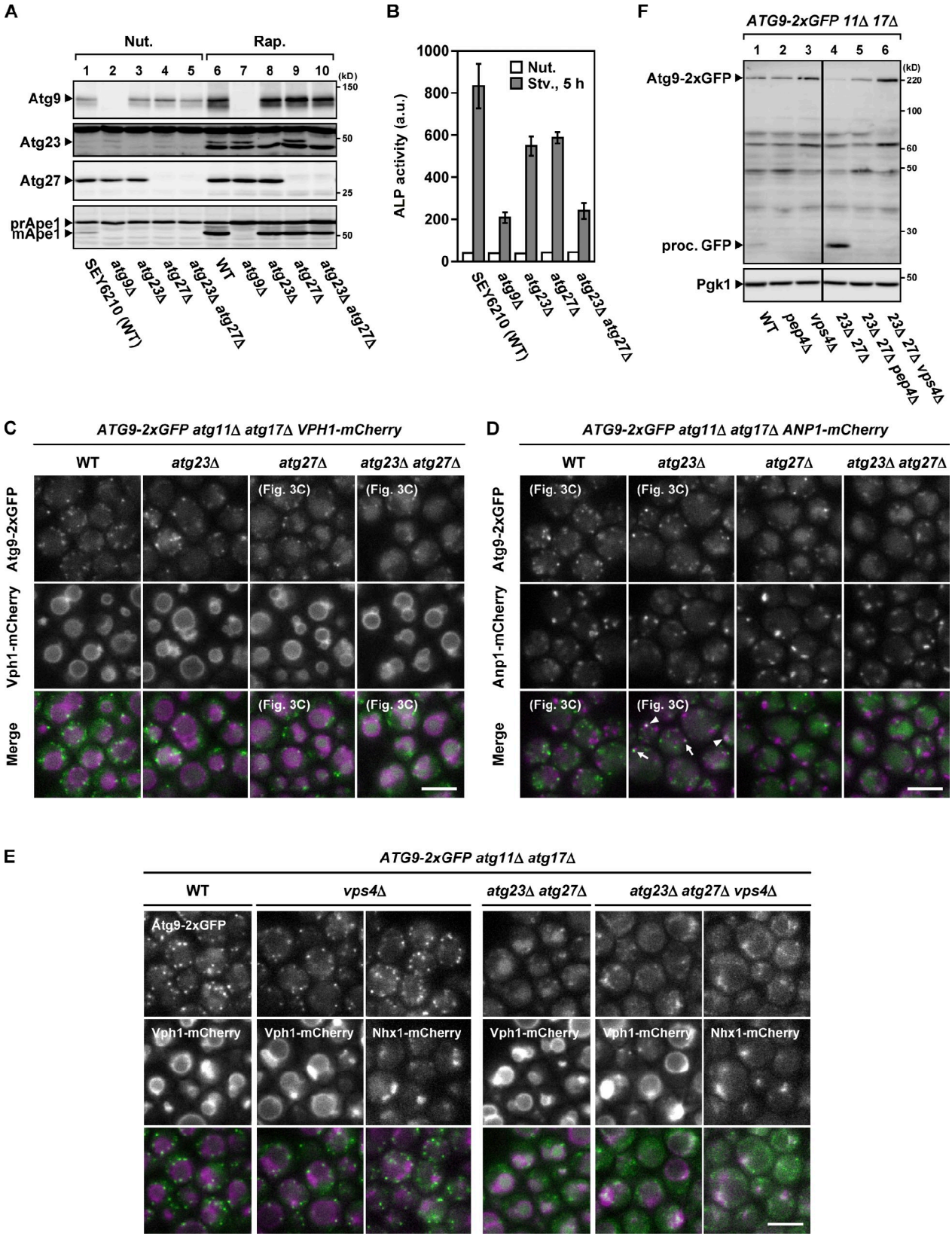

Figure S3. **Atg9 vesicles are derived from the Golgi apparatus in a process involving Atg23 and Atg27.** (A) SEY6210 wild-type cells, *atg9Δ* cells, *atg23Δ* cells, *atg27Δ* cells, and *atg23Δ atg27Δ* cells were grown in SD/CA medium (nutrient [Nut.]) and then treated with rapamycin for 2 h (Rap.). Total cell lysates were prepared from the cells and then subjected to immunoblotting. (B) Autophagic activities of the cells used in A were measured by ALP assay using pTN3 (Noda et al., 1995). Error bars indicate standard deviation. Stv., starved. (C and D) Additional data associated with Fig. 3 C. *ATG9-2×GFP atg11Δ atg17Δ* cells lacking Atg23 and/or Atg27 were treated with rapamycin for 3 h. Several images are also used in Fig. 3 C. Vph1-mCherry (vacuole) and Anp1-mCherry (Golgi) were used as organelle markers. Green fluorescence and red fluorescence were acquired concurrently. Arrowheads and arrows indicate Atg9-GFP clusters accumulated at and adjacent to the Golgi apparatus, respectively. (E) *ATG9-2×GFP atg11Δ atg17Δ* cells lacking Atg23, Atg27, and/or Vps4 were treated with rapamycin for 3 h. Vph1-mCherry (vacuole) and Nhx1-mCherry (endosome) were used as organelle markers. (F) *ATG9-2×GFP atg11Δ atg17Δ* cells lacking Pep4 or Vps4 and *ATG9-2×GFP atg11Δ atg17Δ atg23Δ atg27Δ* cells lacking Pep4 or Vps4 were grown in SD/CA medium and then treated with rapamycin for 3 h. Total cell lysates were prepared from the cells and then subjected to immunoblotting. proc. GFP, the processed form of GFP moiety; WT, wild type. Bars, 5 μm.

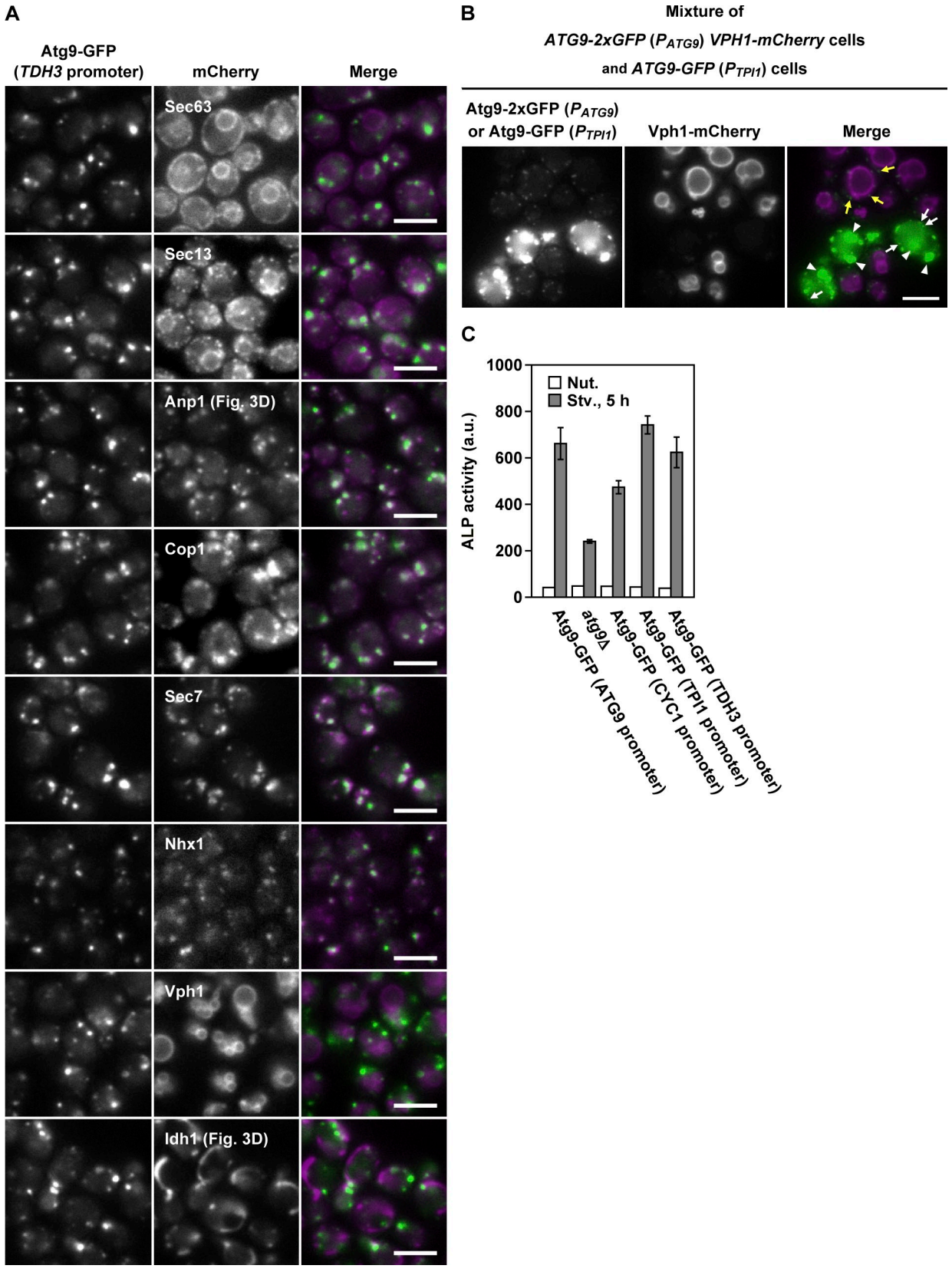

Figure S4. **Overexpressed Atg9 aberrantly accumulates at the Golgi apparatus.** (A) Cells expressing Atg9-GFP via the *TDH3* promoter were observed at 32 ms/frame. Sec63-mCherry (ER), Sec13-mCherry (ER exit site), Anp1-mCherry (Golgi), Cop1-mCherry (Golgi), Sec7-mCherry (trans-Golgi network), Nhx1-mCherry (endosome), Vph1-mCherry (vacuole), and Idh1-mCherry (mitochondria) were used as organelle markers. Anp1-mCherry and Idh1-mCherry are also shown in Fig. 3 D. (B) Cells labeled with Vph1-mCherry expressing Atg9-2×GFP under control of the *ATG9* promoter were mixed with cells expressing Atg9-GFP under control of the *TPI1* promoter and treated with rapamycin for 2 h. Yellow arrows, mobile Atg9 vesicles in cells expressing Atg9-2×GFP under control of the *ATG9* promoter; white arrows, mobile Atg9 vesicles in cells expressing Atg9-GFP under control of the *TPI1* promoter. White arrowheads indicate immobile Atg9-GFP clusters accumulated at the Golgi apparatus in cells expressing Atg9-GFP under control of the *TPI1* promoter. (C) Autophagic activities of the cells used in B were measured by ALP assay using pTN3 (Noda et al., 1995). Error bars indicate standard deviation. (B and C) Even in cells overexpressing Atg9-GFP, a significant number of mobile Atg9 vesicles were still observed in addition to the immobile Atg9 clusters accumulated at the Golgi apparatus, which may explain why these cells exhibit normal autophagic activities. a.u., arbitrary unit; Nut., nutrient; Stv., starved. Bars, 5 µm.

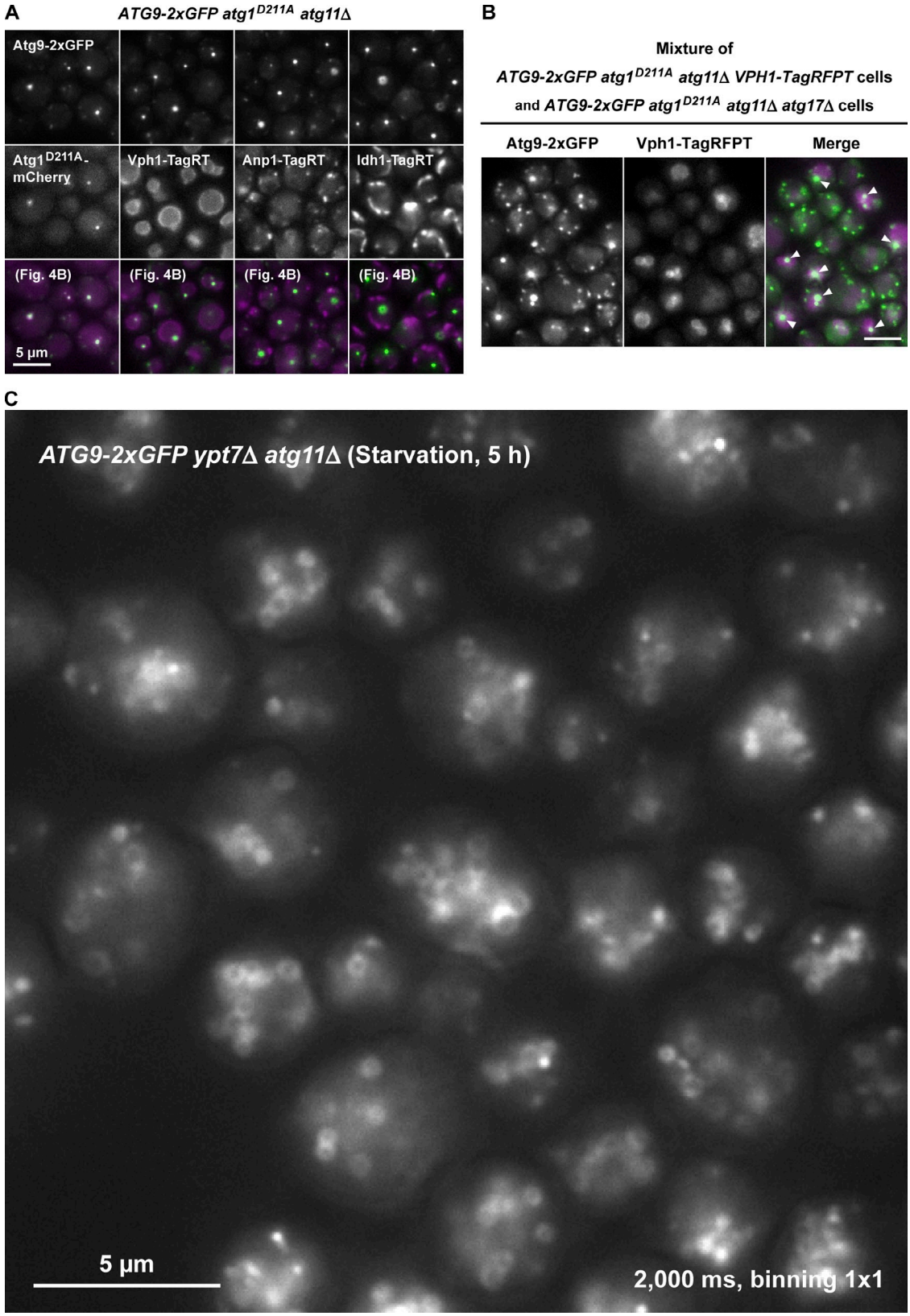

Figure S5. **Atg9 accumulates at the PAS in *atg1* kinase-dead cells and localizes around the autophagosome in *ypt7Δ* cells.** (A) Additional data associated with Fig. 4 B. *ATG9-2×GFP atg1^{D211A} atg11Δ* cells were treated with rapamycin for 1 h. Several images are also used in Fig. 4 B. Atg1^{D211A}-mCherry (PAS), Vph1-TagRFPT (vacuole), Anp1-TagRFPT (Golgi), and Idh1-TagRFPT (mitochondria) were used as organelle markers. (B) The cells used in Fig. 4 A (*ATG9-2×GFP atg1^{D211A} atg11Δ VPH1-TagRFPT* cells and *ATG9-2×GFP atg1^{D211A} atg11Δ atg17Δ* cells) were mixed and starved for 1 h. Arrowheads indicate Atg9-2×GFP vesicles that accumulated at the PAS in *atg1^{D211A} atg11Δ* cells labeled with Vph1-TagRFPT. The vast majority of Atg9 vesicles accumulated at the PAS; accordingly, the number of cytoplasmic mobile Atg9 vesicles was significantly decreased (see also Video 7). Furthermore, in *atg11Δ atg17Δ* cells deficient for PAS formation, Atg9 vesicles were still mobile even under starvation conditions (see also Video 7). Bar, 5 μm. (C) *ATG9-2×GFP ypt7Δ atg11Δ* cells were starved for 5 h in SD(–N) medium to cause autophagosomes to accumulate and then shifted to nutrient-rich SD/CA medium and incubated for 15 min. Cells were observed by fluorescence microscopy at 2,000 ms/frame. The ring-shaped pattern of Atg9-2×GFP was observed in almost all cells.

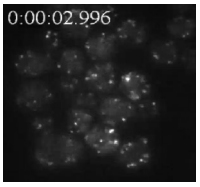

Video 1. **Atg9 vesicles were highly mobile in the cytoplasm.** *ATG9-2×GFP atg11Δ atg17Δ* cells were treated with rapamycin for 3 h. Images were analyzed by time-lapse microscopy at 20 ms/frame using an inverted microscope (IX71). The numbers at the top left indicate seconds and milliseconds.

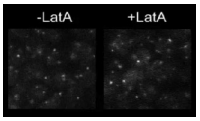

Video 2. **The motion of Atg9 vesicles was not altered after the treatment with latrunculin A.** *ATG9-2×GFP ABP140-mCherry* cells were treated with 100 µg/ml latrunculin A (LatA) for 20 min. Images were analyzed by time-lapse microscopy at 32 ms/frame using an inverted microscope (IX71).

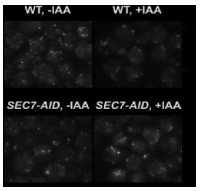

Video 3. **Accumulation of Atg9 at the Golgi apparatus in cells depleted of Sec7.** Video associated with Fig. S2 A. *ATG9-2×GFP DRS2-TagRFPT* cells and *ATG9-2×GFP DRS2-TagRFPT SEC7-AID* cells were treated with rapamycin for 30 min and then with 500 µg/ml IAA for 1 h. Images were analyzed by time-lapse microscopy at 32 ms/frame using an inverted microscope (IX71). In *ATG9-2×GFP DRS2-TagRFPT SEC7-AID* cells treated with IAA, Atg9-2×GFP formed immobile structures. WT, wild type.

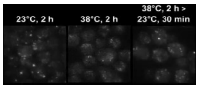

Video 4. **Accumulation of Atg9 at the Golgi apparatus in *sec7*^{ts} cells.** Video associated with Fig. S2 C. *ATG9-2×GFP DRS2-TagRFPT sec7*^{ts} cells grown at 23°C were shifted to 38°C and incubated for 2 h. Next, the cells were shifted to 23°C and incubated for 30 min. Images were analyzed by time-lapse microscopy at 32 ms/frame using an inverted microscope (IX71). At the nonpermissive temperature (38°C), Atg9-2×GFP formed immobile structures.

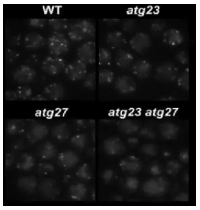

Video 5. **Mislocalization of Atg9 in *atg23Δ* or *atg27Δ* cells.** Video associated with Fig. 3 C. *ATG9-2×GFP atg11Δ atg17Δ* cells lacking Atg23 and/or Atg27 were treated with rapamycin for 3 h. Images were analyzed by time-lapse microscopy at 32 ms/frame using an inverted microscope (IX71). WT, wild type.

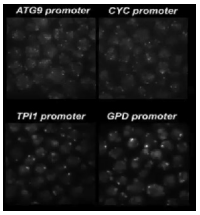

Video 6. **Aberrant accumulation of Atg9 in cells overexpressing Atg9.** Video associated with Fig. 3 E. Cells expressing Atg9-GFP via the *ATG9* promoter, *CYC1* promoter, *TPI1* promoter, or *TDH3* promoter were analyzed by time-lapse microscopy at 32 ms/frame using an inverted microscope (IX71).

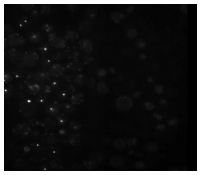

Video 7. **In response to starvation, cytoplasmic Atg9 vesicles assembled to the PAS.** Video associated with Fig. S5 B. *ATG9-2×GFP atg1^{D211A} atg11Δ VPH1-TagRFPT* cells and *ATG9-2×GFP atg1^{D211A} atg11Δ atg17Δ* cells were mixed and then treated with rapamycin for 2 h. Images were analyzed by time-lapse microscopy at 30 ms/frame using an inverted microscope (IX71). In *atg1^{D211A} atg11Δ VPH1-TagRFPT* cells, Atg9-2×GFP vesicles accumulated at the PAS, and the number of cytoplasmic mobile Atg9 vesicles was decreased. Furthermore, no large clusters were observed in *atg1^{D211A} atg11Δ atg17Δ* cells.

Video 8. **Atg9 vesicles assembled individually to the PAS.** Video associated with Fig. 4 C. *ATG9-2×GFP atg1^{D211A}-mCherry atg11Δ* cells were treated with rapamycin for 1 h. Images were analyzed by time-lapse microscopy at 32 ms/frame using an inverted microscope (IX71).

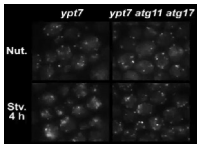

Video 9. **Atg9 localized onto the autophagosomal membranes.** Video associated with Fig. 4 D. *ATG9-2×GFP ypt7Δ* cells and *ATG9-2×GFP ypt7Δ atg11Δ atg17Δ* cells were starved for 4 h. Images were analyzed by time-lapse microscopy at 32 ms/frame using an inverted microscope (IX71). Nut., nutrient; Stv., starved.

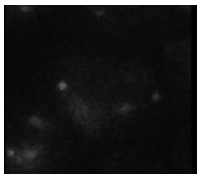

Video 10. **The intensity of Atg9-2×GFP clusters on the autophagosomal membrane was apparently comparable to that of the cytoplasmic mobile Atg9-2×GFP vesicles.** *ATG9-2×GFP ypt7Δ atg11Δ* cells used in Fig. 6 D were starved for 3 h in SD(–N) medium. Images were analyzed by time-lapse microscopy at 30 ms/frame using an inverted microscope (IX71). The intensities of clusters on the autophagosomal membrane were apparently comparable to those of the cytoplasmic mobile Atg9 vesicles.

Table S1. ***S. cerevisiae* strains used in this study**

Strain	Genotype	Source
SEY6210	*MATα ura3-52 his3-200 leu2-3,112 trp1-901 lys2-801 suc2-9*	Darsow et al., 1997
ScHY-188	SEY6210, *ATG9-2×GFP::kanMX6 atg1(D211A)-mCherry::CgTRP1 atg11Δ::CgHIS3*	This study
ScHY-312	SEY6210, *atg9Δ::natNT2*	This study
ScHY-406	SEY6210, *ypt7Δ::natNT2*	This study
ScHY-409	SEY6210, *ATG9-2×GFP::kanMX6 ypt7Δ::natNT2 atg11Δ::CgHIS3*	This study
ScHY-428	SEY6210, *ATG9-2×GFP::kanMX6 ypt7Δ::natNT2 atg11Δ::CgHIS3 atg17Δ::hphNT1*	This study
ScHY-478	SEY6210, *ypt7Δ::natNT2* pRS316[*GFP-ATG8*]	This study
ScHY-482	SEY6210, *atg23Δ::hphNT1*	This study
ScHY-518	SEY6210, *ypt7Δ::natNT2 atg1Δ::hphNT1 atg11Δ::CgHIS3*	This study
ScHY-573	SEY6210, *atg27Δ::hphNT1*	This study
ScHY-737	SEY6210, *leu2Δ::GFP-ATG8::hphNT1 ypt7Δ::natNT2*	This study
ScHY-740	SEY6210, *ATG9-6×HA::kanMX6 ypt7Δ::natNT2*	This study
ScHY-800	SEY6210, *ypt7Δ::natNT2 atg1Δ::kanMX6*	This study
ScHY-858	SEY6210, *ATG9-2×GFP::kanMX6*	This study
ScHY-859	SEY6210, *ATG9-2×GFP::kanMX6 atg1(D211A)::hphNT1*	This study
ScHY-882	SEY6210, *ATG9-2×GFP::kanMX6 atg11Δ::CgHIS3 atg17Δ::hphNT1*	This study
ScHY-917	SEY6210, *ATG9-2×GFP::kanMX6 atg11Δ::CgHIS3 atg17Δ::hphNT1 atg23Δ::natNT2*	This study
ScHY-919	SEY6210, *ATG9-2×GFP::kanMX6 atg11Δ::CgHIS3 atg17Δ::hphNT1 atg27Δ::natNT2*	This study
ScHY-966	SEY6210, *ATG9-GFP::kanMX6*	This study
ScHY-967	SEY6210, P_{TDH3} *(natNT2)-ATG9-GFP::kanMX6*	This study
ScHY-969	SEY6210, P_{CYC1} *(natNT2)-ATG9-GFP::kanMX6*	This study
ScHY-1081	SEY6210, *ATG9-2×GFP::kanMX6 atg11Δ::CgHIS3 ypt7Δ::mCherry-ATG8::zeoNT3*	This study
ScHY-1086	SEY6210, *ATG9-2×Kaede::kanMX6*	This study
ScHY-1087	SEY6210, *ATG9-2×Kaede::kanMX6 atg11Δ::CgHIS3 atg17Δ::hphNT1*	This study
ScHY-1104	SEY6210, P_{TDH3} *(natNT2)-ATG9-GFP::kanMX6 SEC63-mCherry::hphNT1*	This study
ScHY-1105	SEY6210, P_{TDH3} *(natNT2)-ATG9-GFP::kanMX6 SEC13-mCherry::hphNT1*	This study
ScHY-1106	SEY6210, P_{TDH3} *(natNT2)-ATG9-GFP::kanMX6 COP1-mCherry::hphNT1*	This study
ScHY-1107	SEY6210, P_{TDH3} *(natNT2)-ATG9-GFP::kanMX6 ANP1-mCherry::hphNT1*	This study
ScHY-1108	SEY6210, P_{TDH3} *(natNT2)-ATG9-GFP::kanMX6 SEC7-mCherry::hphNT1*	This study
ScHY-1113	SEY6210, P_{TDH3} *(natNT2)-ATG9-GFP::kanMX6 IDH1-mCherry::hphNT1*	This study
ScHY-1114	SEY6210, P_{TDH3} *(natNT2)-ATG9-GFP::kanMX6 VPH1-mCherry::hphNT1*	This study
ScHY-1131	SEY6210, *ATG9-2×GFP::kanMX6 atg11Δ::CgHIS3 atg17Δ::zeoNT3 ANP1-mCherry::hphNT1*	This study
ScHY-1132	SEY6210, *ATG9-2×GFP::kanMX6 atg11Δ::CgHIS3 atg17Δ::zeoNT3 atg23Δ::natNT2 ANP1-mCherry::hphNT1*	This study
ScHY-1133	SEY6210, *ATG9-2×GFP::kanMX6 atg11Δ::CgHIS3 atg17Δ::zeoNT3 atg27Δ::natNT2 ANP1-mCherry::hphNT1*	This study
ScHY-1142	SEY6210, *ATG9-3×BAP::kanMX6 pep4Δ::CgHIS3 leu2Δ::BirA::hphNT1* pRS316[*ATG9-6×FLAG*]	This study
ScHY-1147	SEY6210, *ATG9-2×GFP::kanMX6 VPH1-mCherry::hphNT1*	This study
ScHY-1148	SEY6210, *ATG9-2×GFP::kanMX6 atg11Δ::CgHIS3 atg17Δ::zeoNT3 VPH1-mCherry::hphNT1*	This study
ScHY-1151	SEY6210, *ATG9-2×GFP::kanMX6 atg11Δ::CgHIS3 atg17Δ::zeoNT3 atg23Δ::natNT2 VPH1-mCherry::hphNT1*	This study
ScHY-1154	SEY6210, *ATG9-2×GFP::kanMX6 atg11Δ::CgHIS3 atg17Δ::zeoNT3 atg27Δ::natNT2 VPH1-mCherry::hphNT1*	This study
ScHY-1168	SEY6210, *atg23Δ::hphNT1 atg27Δ::natNT2*	This study
ScHY-1169	SEY6210, *ATG9-2×GFP::kanMX6 atg11Δ::CgHIS3 atg17Δ::zeoNT3 atg23Δ::natNT2 atg27Δ::hphNT1*	This study
ScHY-1176	SEY6210, *ATG9-2×GFP::kanMX6 atg1(D211A)::hphNT1 atg11Δ::CgHIS3 VPH1-TagRFPT::natNT2*	This study
ScHY-1177	SEY6210, *ATG9-2×GFP::kanMX6 atg1(D211A)::hphNT1 atg11Δ::CgHIS3 atg17Δ::natNT2*	This study
ScHY-1220	SEY6210, *pep4Δ::natNT2* pRS316[*ATG9-6×FLAG*]	This study
ScHY-1225	SEY6210, *pep4Δ::natNT2 atg11Δ::CgHIS3 atg17Δ::hphNT1* pRS316[*ATG9*]	This study
ScHY-1226	SEY6210, *pep4Δ::natNT2 atg11Δ::CgHIS3 atg17Δ::hphNT1* pRS316[*ATG9-6×FLAG*]	This study
ScHY-1247	SEY6210, *CSE4-GFP::kanMX6*	This study
ScHY-1260	SEY6210, *ATG9-2×GFP::kanMX6 atg11Δ::CgHIS3 atg17Δ::zeoNT3 atg23Δ::natNT2 atg27Δ::CgTRP1 ANP1-mCherry::hphNT1*	This study
ScHY-1277	SEY6210, *ATG9-2×GFP::kanMX6 leu2Δ::mRFP-APE1::LEU2*	This study
ScHY-1304	SEY6210, P_{TPI1} *(hphNT1)-ATG9-GFP::kanMX6*	This study
ScHY-1309	SEY6210, *ATG9-2×GFP::kanMX6 ATG17-2×mCherry::hphNT1*	This study
ScHY-1311	SEY6210, *ATG9-2×GFP::kanMX6 atg11Δ::CgHIS3 atg17Δ::zeoNT3 IDH1-mCherry::hphNT1*	This study
ScHY-1338	SEY6210, P_{TDH3} *(natNT2)-ATG9-GFP::kanMX6 NHX1-mCherry::hphNT1*	This study
ScHY-1429	SEY6210, *ATG9-2×GFP::kanMX6 pep4Δ::natNT2 atg11Δ::CgHIS3 atg17Δ::hphNT1*	This study

Table S1. ***S. cerevisiae* strains used in this study** *(Continued)*

Strain	Genotype	Source
ScHY-1660	SEY6210, *leu2Δ::GFP-ATG8::hphNT1 atg11Δ::kanMX6 atg17Δ::zeoNT3 ypt7Δ::natNT2*	This study
ScHY-1925	SEY6210, *ATG9-2×GFP::kanMX6 atg11Δ::CgHIS3 atg17Δ::zeoNT3 atg23Δ::natNT2 atg27Δ::CgTRP1 VPH1-mCherry::hphNT1*	This study
ScHY-1928	SEY6210, *ANP1-GFP::kanMX6 pep4Δ::natNT2 atg11Δ::CgHIS3 atg17Δ::hphNT1*	This study
ScHY-1933	SEY6210, *atg8Δ::GFP-ATG8::hphNT1 leu2Δ::mRFP-APE1::LEU2*	This study
ScHY-1935	SEY6210, *pep4Δ::natNT2* pRS316[*ATG9*]	This study
ScHY-1947	SEY6210, *ATG9-2×GFP::kanMX6 atg11Δ::CgHIS3 atg17Δ::zeoNT3 vps4Δ::natNT2 VPH1-mCherry::hphNT1*	This study
ScHY-1951	SEY6210, *ATG9-2×GFP::kanMX6 atg11Δ::CgHIS3 atg17Δ::zeoNT3 atg23Δ::KlURA3 atg27Δ::CgTRP1 vps4Δ::natNT2 VPH1-mCherry::hphNT1*	This study
ScHY-2019	SEY6210, *ATG9-2×GFP::kanMX6 atg1(D211A)::hphNT1 atg11Δ::CgHIS3 ANP1-TagRFPT::natNT2*	This study
ScHY-2020	SEY6210, *ATG9-2×GFP::kanMX6 atg1(D211A)::hphNT1 atg11Δ::CgHIS3 IDH1-TagRFPT::natNT2*	This study
ScHY-2062	X2180, *sec7(ts) ATG9-2×GFP::natNT2 DRS2-TagRFPT::hphNT1*	This study
ScHY-2076	W303-1A, *ATG9-2×GFP::kanMX6* P_{ADH} *-OsTIR1-9×Myc::URA3 ade2::ADE2 GRS2-TagRFPT::hphNT1*	This study
ScHY-2077	W303-1A, *ATG9-2×GFP::kanMX6* P_{ADH} *-OsTIR1-9×Myc::URA3 ade2::ADE2 SEC7-AID::natNT2 GRS2-TagRFPT::hphNT1*	This study
ScHY-2388	SEY6210, *ATG9-2×GFP::kanMX6 atg11Δ::CgHIS3 atg17Δ::hphNT1 vps4Δ::natNT2*	This study
ScHY-2389	SEY6210, *ATG9-2×GFP::kanMX6 atg11Δ::CgHIS3 atg17Δ::zeoNT3 atg23Δ::KlURA3 atg27Δ::hphNT1 vps4Δ::natNT2*	This study
ScHY-2390	SEY6210, *ATG9-2×GFP::kanMX6 atg11Δ::CgHIS3 atg17Δ::zeoNT3 atg23Δ::KlURA3 atg27Δ::hphNT1 pep4Δ::natNT2*	This study
ScHY-2393	SEY6210, *ATG9-2×GFP::kanMX6 atg11Δ::CgHIS3 atg17Δ::zeoNT3 NHX1-mCherry::hphNT1*	This study
ScHY-2394	SEY6210, *ATG9-2×GFP::kanMX6 atg11Δ::CgHIS3 atg17Δ::zeoNT3 vps4Δ::natNT2 NHX1-mCherry::hphNT1*	This study
ScHY-2395	SEY6210, *ATG9-2×GFP::kanMX6 atg11Δ::CgHIS3 atg17Δ::zeoNT3 atg23Δ::KlURA3 atg27Δ::CgTRP1 vps4Δ::natNT2 NHX1-mCherry::hphNT1*	This study
ScHY-2412	SEY6210, *ATG9-2×GFP::kanMX6 atg11Δ::CgHIS3 atg17Δ::zeoNT3 ABP140-mCherry::hphNT1*	This study

References

Darsow, T., S.E. Rieder, and S.D. Emr. 1997. A multispecificity syntaxin homologue, Vam3p, essential for autophagic and biosynthetic protein transport to the vacuole. *J. Cell Biol.* 138:517–529. http://dx.doi.org/10.1083/jcb.138.3.517

Franzusoff, A., and R. Schekman. 1989. Functional compartments of the yeast Golgi apparatus are defined by the *sec7* mutation. *EMBO J.* 8:2695–2702.

Mari, M., J. Griffith, E. Rieter, L. Krishnappa, D.J. Klionsky, and F. Reggiori. 2010. An Atg9-containing compartment that functions in the early steps of autophagosome biogenesis. *J. Cell Biol.* 190:1005–1022. http://dx.doi.org/10.1083/jcb.200912089

Nishimura, K., T. Fukagawa, H. Takisawa, T. Kakimoto, and M. Kanemaki. 2009. An auxin-based degron system for the rapid depletion of proteins in nonplant cells. *Nat. Methods*. 6:917–922. http://dx.doi.org/10.1038/nmeth.1401

Noda, T., A. Matsuura, Y. Wada, and Y. Ohsumi. 1995. Novel system for monitoring autophagy in the yeast *Saccharomyces cerevisiae*. *Biochem. Biophys. Res. Commun.* 210:126–132. http://dx.doi.org/10.1006/bbrc.1995.1636

Novick, P., C. Field, and R. Schekman. 1980. Identification of 23 complementation groups required for post-translational events in the yeast secretory pathway. *Cell*. 21:205–215. http://dx.doi.org/10.1016/0092-8674(80)90128-2

Ohashi, Y., and S. Munro. 2010. Membrane delivery to the yeast autophagosome from the Golgi-endosomal system. *Mol. Biol. Cell*. 21:3998–4008. http://dx.doi.org/10.1091/mbc.E10-05-0457